

Distance between collapsing matter and trapping horizon in evaporating black holes

Pei-Ming Ho^{a†}, Yoshinori Matsuo^{b‡} and Yuki Yokokura^{c§}

^a *Department of Physics and Center for Theoretical Physics,
National Taiwan University, Taipei 106, Taiwan, R.O.C.*

^b *Department of Physics, Osaka University,
Toyonaka, Osaka 560-0043, Japan*

^c *iTHEMS Program, RIKEN, Wako, Saitama 351-0198, Japan*

Abstract

Assuming that the vacuum energy-momentum tensor is not exceptionally large, we give a general proof for 4D evaporating black holes with spherical symmetry that the surface of the collapsing matter can never be farther inside the timelike trapping horizon than a proper distance $\sim \mathcal{O}(n^{3/2}\ell_p)$ when the black hole is evaporated to $1/n$ of its initial mass, as long as $n \ll a^{2/3}/\ell_p^{2/3}$ (where a is the Schwarzschild radius and ℓ_p is the Planck length). For example, the distance between the matter and the apparent horizon must be Planckian at the Page time.

[†]e-mail: pmho@phys.ntu.edu.tw

[‡]e-mail: matsuo@het.phys.sci.osaka-u.ac.jp

[§]e-mail: yuki.yokokura@riken.jp

1 Introduction

It was emphasized in Ref. [1] that, if the information paradox of black holes is resolved by converting all information of the collapsing matter (say, the information inside nuclei) into the Hawking radiation, there should be high-energy events around the horizon (such as the firewall [2, 3]). However, if the collapsing matter is already far inside the horizon, even a firewall around the horizon is still not enough unless there are some large-scale nonlocal interactions at work.

According to the conventional model of the quantum energy-momentum tensor around an evaporating black hole [4–6], an ingoing negative energy flow appears near the Schwarzschild radius, which leads to the presence of the timelike apparent horizon [17]. The collapsing matter can get inside the apparent horizon, and it would be interesting to know the relative position of the collapsing matter and the apparent horizon after that. The question we want to answer in this paper is the following: How far is the collapsing matter under the apparent horizon when the black hole evaporates to a certain fraction of its initial mass, say, one half at the Page time?

For 4D spherically symmetric evaporating black holes, we consider a generic class of vacuum energy-momentum tensor without exceptionally large components, and prove that, due to a robust exponential form of the redshift factor inside the timelike trapping horizon, the proper distance between the timelike trapping horizon and the collapsing matter is never larger than $n^{3/2}\ell_p$ when the black hole is $1/n$ of its initial mass. This estimate is valid until the black-hole mass is an extremely small fraction $1/n \sim \mathcal{O}(\ell_p^{2/3}/a^{2/3})$ of its initial mass.¹

2 Assumptions

In this paper, we make the following assumptions.

1. Macroscopic evaporating black hole

To justify the use of the semi-classical Einstein equation and low-energy effective theories for matter, we assume that the Schwarzschild radius is much larger than the Planck length:

$$\ell_p \ll a(t), \quad (2.1)$$

where $a(t) \equiv 2G_N M(t)$ is the Schwarzschild radius for a black hole of mass $M(t)$ (where $G_N = \ell_p^2/\hbar$ is the Newton constant). This justifies the perturbative expansion in ℓ_p^2/a^2 .

The time-evolution equation for $a(t)$ is roughly given by

$$\dot{a} \sim -\ell_p^2/a^2, \quad (2.2)$$

¹ For the vacuum energy-momentum tensor defined by a 2D massless scalar field [4], the Planck-scale proper distance between trapping horizon and collapsing matter was already argued in Ref. [7].

for the time t of a fiducial observer far from the black hole, so that the time for the black hole to evaporate to a fraction ($< 1/2$) of its initial mass is $\mathcal{O}(a^3/\ell_p^2)$.² Here we are concerned with an extremely long elapse of time $\Delta t \sim \mathcal{O}(a^3/\ell_p^2)$.

2. Spherical symmetry

For simplicity, we assume spherical symmetry. The most general spherically symmetric 4D metric is

$$ds^2 = -C(u, v)dudv + r^2(u, v)d\Omega^2, \quad (2.3)$$

where u and v are the outgoing and ingoing light-cone coordinates, $r(u, v)$ is the areal radius and $d\Omega^2$ is the metric of a unit 2-sphere.

3. Semi-classical Einstein equation

The semi-classical Einstein equation

$$G_{\mu\nu} = \kappa \langle T_{\mu\nu} \rangle \quad (2.4)$$

is assumed to hold since we will focus only on spacetime regions where the curvature is small. Here, $\kappa \equiv 8\pi G_N$ and $\langle T_{\mu\nu} \rangle$ is the expectation value of the quantum energy-momentum tensor operator for a given quantum state in a certain quantum field theory. Since the quantum effect $\langle T_{\mu\nu} \rangle$ is proportional to the Planck constant \hbar , the quantum correction to the Einstein equation is proportional to $\mathcal{O}(\ell_p^2)$.

4. Schwarzschild approximation

Since the Hawking radiation is extremely weak, within a time $\Delta t \sim \mathcal{O}(a)$ (see eq.(2.2)), the spacetime geometry is well approximated by the Schwarzschild solution outside the trapping horizon where

$$r - a \gg \mathcal{O}\left(\frac{\ell_p^2}{a}\right). \quad (2.5)$$

The more precise mathematical statement of this assumption will be given in Sec.3.

5. Bounds on energy-momentum tensor

We shall assume that the energy-momentum tensor in the near-horizon region³ does not violate the inequalities:

$$\langle T^\mu{}_\mu \rangle \lesssim \mathcal{O}\left(\frac{1}{\kappa a^2}\right), \quad (2.6)$$

$$\langle T^\theta{}_\theta \rangle \lesssim \mathcal{O}\left(\frac{1}{\kappa a^2}\right). \quad (2.7)$$

² As an example, $\ell_p^2/a_\odot^2 \sim 10^{-76}$ for the Schwarzschild radius a_\odot of the sun.

³ The precise definition of the ‘‘near-horizon region’’ will be given in Sec.(4.1).

These bounds are much weaker than those of the conventional model [4–6], for which $\langle T^\mu{}_\mu \rangle \sim \mathcal{O}(\hbar/a^4)$ is fixed by the conformal anomaly ⁴. These conditions also imply that the curvature is not exceptionally large, no larger than $\mathcal{O}(1/a^2)$.

6. Trapping horizon

The trapping horizon is the boundary of a trapped region, hence $\partial_v r(u, v) = 0$ on the trapping horizon. (A spacelike slice of the trapping horizon is called the apparent horizon.) It is often considered as a replacement of the notion of the event horizon for dynamical black-holes [11–13], since the event horizon is defined by the global structure of the spacetime, which will be irrelevant to the local dynamical geometry. We will be concerned with the timelike branch of the outer trapping horizon. (See Fig.1.)

This part of the trapping horizon is timelike due to the quantum effect of an ingoing negative energy flow [14–17]. For the classical Schwarzschild solution, the trapping horizon and the event horizon are identical, and the areal radius of the event horizon equals the Schwarzschild radius. In dynamical cases, the event horizon and trapping horizon are in general different. The quantum correction, which should be of $\mathcal{O}(\ell_p^2)$ in eq.(2.4), is expected to introduce a small difference between the areal radius of the trapping horizon and the Schwarzschild radius:

$$r(u, v_{ah}(u)) - a(u) \sim \mathcal{O}(\ell_p^2/a). \quad (2.8)$$

Here, $a(u)$ is the u -dependent Schwarzschild radius which decreases with time as (2.2), and we use $u_{ah}(v)$ and $v_{ah}(u)$ to denote the u and v coordinates of the apparent horizon for given v and u , respectively.

3 Schwarzschild Approximation

The near-horizon geometry is expected to deviate from the classical Schwarzschild solution due to the quantum correction. But it should be smoothly connected to the classical metric at large distances. In this section, we study the classical Schwarzschild solution and its behaviour near the horizon that will be used to deduce the boundary condition for the near-horizon geometry in the next section.

We consider the gravitational collapse of classical null matter with spherical symmetry in an asymptotically Minkowski space. We assume that the collapsing matter has a well-defined surface, outside of which the space is in the vacuum state. Over a period of time $\Delta t \sim \mathcal{O}(a^3/\ell_p^2)$, the geometry of the space sufficiently far away from the Schwarzschild radius $a(t)$ should be well approximated by the Schwarzschild metric.

⁴However, these conditions are violated under the surface of the collapsing matter in the model proposed in Ref. [9, 10].

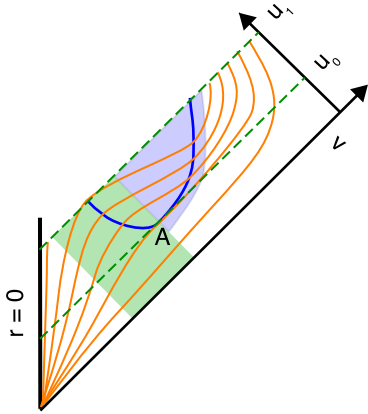


Figure 1: Penrose diagram for the spacetime region of interest (called the *near-horizon region* to be defined in Sec.4.1). A (null) collapsing matter is shown as a thick strip (green), outside of which there is negative incoming energy flow. The trapping horizon (blue curve) is spacelike inside the collapsing matter, timelike outside it, and tangent to the constant- u curve at the point A where its u -coordinate has the minimal value u_0 . The constant- r curves (orange) are tangent to constant- u curves on the trapping horizon. We are not concerned with what happens at the late stage of the black-hole evaporation when the black hole is no longer macroscopic, or when the trapping horizon in vacuum is no longer timelike, so we choose a cutoff time at $u = u_1$. The “near-horizon region” defined in Sec.4.1 is the region (blue shade) bounded by a curve outside but close to the timelike trapping horizon in vacuum, the curve of $u = u_1$ (dashed green), and the outer surface of the collapsing matter.

More precisely, since the position of the apparent horizon with the quantum correction is given by eq.(2.8), the Schwarzschild solution with a time-dependent Schwarzschild radius $a(t)$ should be a good approximation at a place well outside the Schwarzschild radius where

$$r - a \gtrsim \frac{N\ell_p^2}{a} \quad (3.1)$$

with a sufficiently large (but finite) N (e.g. $N \sim 10000$).

In this section, we consider a further approximation as follows. The Schwarzschild radius $a(t)$ changes slowly with time as eq.(2.2), and the change in a is a tiny fraction $\Delta a/a \sim \mathcal{O}(\ell_p^2/a^2)$ over a lapse of time of $\mathcal{O}(a)$ for a distant observer. That is, for a spacetime region of $\Delta t \sim \mathcal{O}(a)$ and $r - a \gtrsim N\ell_p^2/a$ ⁵, the Schwarzschild metric with a constant Schwarzschild radius a is a good approximation.

⁵ Strictly speaking, $r - a \gtrsim N\ell_p^2/a$ can be satisfied both outside and inside the Schwarzschild radius, since the areal radius r has a local minimum at the apparent horizon. In the sentence above, we are referring to the region outside the Schwarzschild radius.

More specifically, we consider the small neighbourhood outside the trapping horizon ⁶

$$r - a \in \left(\frac{N\ell_p^2}{2a}, \frac{N\ell_p^2}{a} \right) \quad (3.2)$$

and a period of time $[t_0, t_0 + \Delta t]$ where $\Delta t \sim \mathcal{O}(a)$. Here, we assume that N is sufficiently large so that the Schwarzschild approximation is good, but at the same time, it should not be too large,

$$\frac{a^2}{\ell_p^2} \gg N \quad (3.3)$$

so that $(r - a)/a \ll 1$. Then, the metric can be approximated as the usual Schwarzschild metric with the constant radius a that corresponds to that at $t = t_0$:

$$ds^2 = - \left(1 - \frac{a}{r(u, v)} \right) dudv + r^2(u, v) d\Omega^2, \quad (3.4)$$

where the areal radius $r(u, v)$ is related to the tortoise coordinate r^* via

$$\begin{aligned} r^* &\equiv \frac{v - u}{2} = r(u, v) + a \log \left(\frac{r(u, v)}{a} - 1 \right) \\ &\simeq a + a \log \left(\frac{r(u, v) - a}{a} \right), \end{aligned} \quad (3.5)$$

due to eqs.(3.2) and (3.3). In the neighbourhood (3.2), therefore, the Schwarzschild metric (3.4) becomes approximately

$$ds^2 \simeq -C_0(u, v) dudv + a^2 d\Omega^2, \quad (3.6)$$

where

$$C_0(u, v) \equiv \frac{a}{r} e^{\frac{v-u-2a}{2a}}. \quad (3.7)$$

In the neighbourhood (3.2), the metric (3.4) means

$$C(u, v) \sim \mathcal{O} \left(\frac{\ell_p^2}{a^2} \right). \quad (3.8)$$

For later use, we introduce $\Sigma(u, v)$ as

$$C(u, v) \equiv \frac{e^{\Sigma(u, v)}}{r(u, v)}. \quad (3.9)$$

Then, Σ_0 , which is defined by $C_0 = e^{\Sigma_0}/r$, is

$$\Sigma_0(u, v) \simeq \frac{v - u}{2a} - 1 + \log(a). \quad (3.10)$$

In the above discussion, we have suppressed the u -dependence of the Schwarzschild radius $a(u)$ because we will apply these expressions only to short periods of time $\lesssim \mathcal{O}(a)$.

⁶ The choice of the domain $\left(\frac{N\ell_p^2}{2a}, \frac{N\ell_p^2}{a} \right)$ is arbitrary, as long as it covers a neighbourhood of eq.(3.1) where the Schwarzschild approximation is good.

4 Solving Semi-Classical Einstein Equations

In this section, we consider the vacuum energy-momentum tensor satisfying eqs.(2.6) and (2.7), solve the Einstein equation (2.4) and obtain a robust form of $C(u, v)$.⁷

4.1 Near-Horizon Region

In this work, we use the phrase *near-horizon region* to refer to a region of spacetime defined as the interior space of the following three hypersurfaces. See Fig.1. The first of the hypersurfaces is the timelike 3D trajectory of the 2-sphere which defines the outer boundary of the near-horizon region. It must be outside the trapping horizon (2.8) where the classical approximation in the previous section should be valid around it. Thus we choose the outer boundary of the near-horizon region (for convenience) to coincide with the outer boundary of the neighbourhood (3.2),

$$r(u, v) - a(u) = \frac{N\ell_p^2}{a(u)}. \quad (4.1)$$

The 2nd hypersurface is the outer surface of the null collapsing matter, whose areal radius is denoted by $R_s(u)$. The 3rd is the upper bound of the retarded time $u = u_1$, which is chosen to cut off the late stage of the evaporation when the trapping horizon in vacuum turns spacelike. For $u < u_1$, $R_s(u)$ and $a(u)$ are assumed to be much larger than the cutoff length scale of the low-energy effective theory.

We focus our attention on a range of $u \in (u_0, u_1)$, where u_0 is the moment when the trapping horizon emerges. We emphasize that in the near-horizon region, the ranges of u and v are both $\sim \mathcal{O}(a^3/\ell_p^2)$. In terms of the (u, v) coordinates, the near-horizon region defined above covers a huge space.

The Schwarzschild radius $a(u)$ is monotonically decreasing due to Hawking radiation as eq.(2.2). The maximal and minimal values of $a(u)$ from $u = u_0$ to u_1 are given by, respectively,

$$a_{max} = a(u_0) \quad \text{and} \quad a_{min} = a(u_1). \quad (4.2)$$

The ratio of the initial and final mass is denoted by

$$n \equiv \frac{a_{max}}{a_{min}}. \quad (4.3)$$

The trajectory of the outer boundary (4.1) of the near-horizon region can be parameterized either by u or by v . Equivalently, eq.(4.1) gives the relation between u and v on the trajectory. Using u as the parameter, the v -coordinate on the trajectory is obtained as a

⁷For the case of the vacuum energy-momentum tensor based on a 2D massless scalar field [4], the metric functions $C(u, v)$ and $r(u, v)$ in the near-horizon region are solved from the semi-classical Einstein equation in Ref. [7].

function of u by solving (4.1). It is denoted by $v_{out}(u)$, and satisfies eq.(4.1) as

$$r(u, v_{out}(u)) - a(u) = \frac{N\ell_p^2}{a(u)}. \quad (4.4)$$

Conversely, using v as the parameter, its u -coordinate is denoted by $u_{out}(v)$ and eq.(4.1) says that

$$r(u_{out}(v), v) - \bar{a}(v) = \frac{N\ell_p^2}{\bar{a}(v)}, \quad (4.5)$$

where

$$\bar{a}(v) \equiv a(u_{out}(v)). \quad (4.6)$$

Clearly, u_{out} and v_{out} are the inverse functions of each other; $u_{out}(v_{out}(u)) = u$ and $v_{out}(u_{out}(v)) = v$.

Note that, for a point (u, v) inside the trapping horizon, where the position of the trapping horizon for a given value of u or v is specified as $(u, v_{ah}(u))$ or $(u_{ah}(v), v)$ (see (2.8)), respectively, we have

$$v < v_{ah}(u) < v_{out}(u), \quad u > u_{ah}(v) > u_{out}(v), \quad (4.7)$$

since the trapping horizon is timelike and lies inside the outer boundary of the near-horizon region. (See Fig.2.) These inequalities hold because the trapping horizon is timelike, as a result of the quantum effect of a negative vacuum energy flow. ⁸

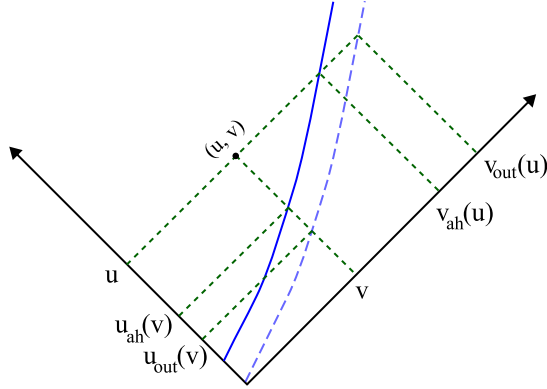


Figure 2: The trapping horizon (solid blue) and the outer boundary of the near-horizon region (dash blue) have their u, v coordinates given by $u_{ah}(v), v_{ah}(u)$ and by $u_{out}(v), v_{out}(u)$, respectively. The coordinates (u, v) of a point inside the trapping horizon satisfy eq.(4.7).

4.2 Solution Of $C(u, v)$

As we will see later, only the function $C(u, v)$ in the metric (2.3) is needed to determine the proper distance between the collapsing matter and the trapping horizon. Here we solve

⁸If we consider a point inside a spacelike trapping horizon, we would have $v > v_{ah}(u)$ and $u > u_{ah}(v)$.

$C(u, v)$ from the semi-classical Einstein equation (2.4) in the near-horizon region, with the boundary condition that it agrees with the Schwarzschild approximation in the neighbourhood (3.2).

Consider a particular combination of the semi-classical Einstein equations

$$G^\mu{}_\mu - 6G^\theta{}_\theta = \kappa (\langle T^\mu{}_\mu \rangle - 6\langle T^\theta{}_\theta \rangle). \quad (4.8)$$

It is equivalent to

$$\partial_u \partial_v \Sigma(u, v) = \frac{C(u, v)}{4r^2(u, v)} + \frac{\kappa C(u, v)}{8} (\langle T^\mu{}_\mu \rangle - 6\langle T^\theta{}_\theta \rangle), \quad (4.9)$$

where $\Sigma(u, v)$ is defined by eq.(3.9). It admits a simple solution at the lowest order.

For $r - a \sim \ell_p^2/a$, the naive order of magnitude of the left-hand side of eq.(4.9) is $\mathcal{O}(1/a^2)$,⁹ and that of the right-hand side is $\mathcal{O}(\ell_p^2/a^4)$ because of eqs.(2.6) and (2.7). Hence, the leading-order approximation of eq.(4.9) is

$$\partial_u \partial_v \Sigma \simeq 0. \quad (4.10)$$

Indeed, in the neighbourhood (3.2) of the outer boundary (4.1) where the Schwarzschild solution is a good approximation, Σ is approximated by Σ_0 (3.10), for which $\partial_u \partial_v \Sigma_0 = 0$. We shall treat the terms on the right-hand side of eq.(4.9) perturbatively, and check later what the range of validity of this perturbative solution is.

Eq.(4.10) is solved by

$$\Sigma(u, v) \simeq B(u) + \bar{B}(v) \quad (4.11)$$

for arbitrary functions $B(u)$ and $\bar{B}(v)$. To determine $B(u)$ and $\bar{B}(v)$, we impose the boundary condition that $C(u, v)$ matches with the Schwarzschild metric (3.7) in the neighbourhood (3.2) around the outer boundary of the near-horizon region. (See Fig.3.)

Consider an arbitrary point (u, v) inside the near-horizon region. (See Fig.3.) According to eq.(4.11), over an infinitesimal variation from u to $(u + du)$ along a constant- v curve, the corresponding change in $\Sigma(u, v)$ is $du \partial_u B(u)$. Since it is independent of v , the quantity $du \partial_u \Sigma(u, v)$ for an arbitrary point (u, v) inside the horizon should be identical to $du \partial_u \Sigma(u, v')$ in the region (3.2) where $\Sigma \simeq \Sigma_0$ (3.10) with, say, $v' = v_{out}(u)$:

$$du \partial_u B(u) \simeq du \partial_u \Sigma(u, v) \simeq du \partial_u \Sigma_0(u, v') \Big|_{v'=v_{out}(u)} \simeq -\frac{du}{2a(u)}. \quad (4.12)$$

Here, we have used (3.10) with $a(u)$ and neglected contributions from $\partial_u a(u)$ as higher-order terms. Since the procedure above can be repeated for each infinitesimal segment du for the same v , the equation above is immediately solved by

$$B(u) \simeq B(u_*) - \int_{u_*}^u \frac{du'}{2a(u')} \quad (4.13)$$

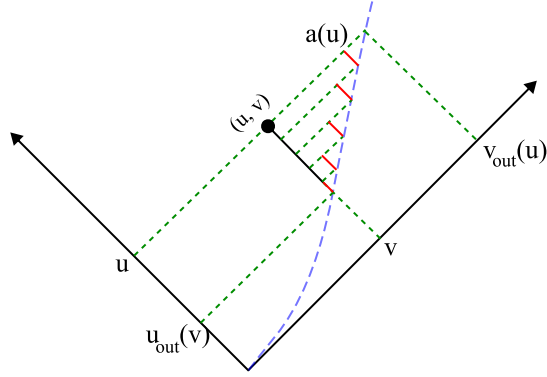


Figure 3: The dash blue curve represents the outer boundary of the near-horizon region. Along the constant- v curve, the u -dependence of Σ must agree with that of Σ_0 in the region (3.2).

for an arbitrary reference point (u_*, v_*) inside the near-horizon region.

Similarly,

$$\bar{B}(v) \simeq \bar{B}(v_*) + \int_{v_*}^v \frac{dv'}{2\bar{a}(v')}. \quad (4.14)$$

According to eqs.(4.13) and (4.14), the 0-th order approximation of $\Sigma(u, v)$ is

$$\Sigma(u, v) \simeq \Sigma(u_*, v_*) - \int_v^{v_*} \frac{dv'}{2\bar{a}(v')} - \int_{u_*}^u \frac{du'}{2a(u')}. \quad (4.15)$$

As a result, we obtain

$$C(u, v) \simeq C(u_*, v_*) \frac{r(u_*, v_*)}{r(u, v)} \exp \left[- \int_{u_*}^u \frac{du'}{2a(u')} - \int_v^{v_*} \frac{dv'}{2\bar{a}(v')} \right]. \quad (4.16)$$

Note that this formula can be applied to any two points (u, v) and (u_*, v_*) inside the near-horizon region.

We shall adopt the convention of choosing (u_*, v_*) to be an arbitrary point on the outer boundary of the near-horizon region. Hence (u_*, v_*) can also be written as $(u_{out}(v_*), v_*)$ or $(u_*, v_{out}(u_*))$. Then, to match with the Schwarzschild solution (3.4) with $a(u)$ in the region (3.2), from eq.(3.8), we have

$$C(u_*, v_*) \sim \mathcal{O}(\ell_p^2/a(u_*)^2). \quad (4.17)$$

In view of eqs.(4.7) and (4.16), $C(u, v)$ becomes exponentially smaller as we go deeper inside the near-horizon region. This is the crucial property of the near-horizon geometry that prevents the distance between the collapsing matter and the trapping horizon from becoming macroscopic until the very late stage of the evaporation.

⁹One can use eqs.(3.4) and (3.5) and estimate $\partial_u \partial_v \Sigma = \partial_u \partial_v C/C - \partial_u C \partial_v C/C^2 + \partial_u \partial_v r/r - \partial_u r \partial_v r/r^2 = \mathcal{O}(1/a^2)$ for $r - a \sim \ell_p^2/a$.

4.3 First-Order Quantum Correction

In this subsection, we check the 1st-order quantum correction of $\Sigma(u, v)$ according to eq.(4.9). Since we consider a large range of both u and v of $\mathcal{O}(a^3/\ell_p^2)$, the approximation (4.10) might break down after the integration over such a large range of u and v . Here, we check that the approximation is valid over this large range of u and v . Due to the exponential factors in $C(u, v)$ (See eq.(4.16)), as we go deeper inside the near-horizon region, $C(u, v)$ becomes exponentially smaller, and hence the approximation of ignoring the right hand side of eq.(4.9) gets better.

To be more precise, the correction to $\Sigma(u, v)$ due to the right-hand side of eq.(4.9) can be computed perturbatively at the 1st order as

$$\begin{aligned} \Delta\Sigma(u, v) &\simeq \int_{u_*}^u du' \int_{v_*}^v dv' \left[\frac{1}{4r^2(u', v')} + \frac{\kappa}{8} (\langle T^\mu{}_\mu \rangle + 2\langle T^\theta{}_\theta \rangle) \right] C(u', v') \\ &\lesssim \left[\frac{1}{4r_{min}^2} + \frac{K}{8a_{min}^2} \right] C(u_*, v_*) \frac{r_{max}}{r_{min}} \int_{u_*}^u du' \int_{v_*}^v dv' e^{-\frac{v_*-v'}{2a_{max}}} e^{-\frac{u'-u_*}{2a_{max}}} \\ &\lesssim \left[\frac{a_{min}^2}{r_{min}^2} + \frac{K}{2} \right] \frac{a_{max}^2}{a_{min}^2} \frac{r_{max}}{r_{min}} C(u_*, v_*), \end{aligned} \quad (4.18)$$

where we have used eq.(4.7) in the last step, and r_{max} and r_{min} denote the maximal and minimal values of $r(u, v)$ in the near-horizon region. We have also assumed that

$$|\langle T^\mu{}_\mu \rangle + 2\langle T^\theta{}_\theta \rangle| \leq \frac{K}{\kappa a^2} \quad (4.19)$$

at any time, and that K is of $\mathcal{O}(1)$ according to our assumptions (2.6), (2.7).

The ratios r_{max}/r_{min} and a_{min}/r_{min} appearing in eq.(4.18) can be estimated without an explicit functional form of $r(u, v)$. First, eqs. (2.8) and (4.4) say that both the areal radius $r(u, v_{ah}(u))$ at the trapping horizon and the areal radius $r(u, v_{out}(u))$ at the outer boundary approximately equal the Schwarzschild radius $a(u)$ up to higher-order terms $\sim \mathcal{O}(\ell_p^2/a)$. This is one of the two principles that govern the basic features of the function $r(u, v)$. The other principle is simply the conditions $\partial_v r(u, v) < 0$ and $\partial_u r(u, v) < 0$, which hold by definition for the trapped region. Therefore, $r(u, v)$ decreases with u for a fixed v . More precisely, $r(u, v)$ on each constant- v curve decreases slower with u for smaller values of v because of the larger red-shift factor for deeper places inside the horizon. Thus, at the outer boundary, the areal radius becomes the maximum on each constant- v curve in the near-horizon region. At the same time, $r(u, v)$ decreases also with v for a fixed u . The minimum of the areal radius on each constant- u curve is that on the trapping horizon.

With the discussion above, we can draw an inspection of Fig.4, which is a point-by-point image of Fig.1 via the coordinate transformation from (u, v) to (r, v) . It should be clear that we can approximate r_{max} and r_{min} , respectively, as the maximal and minimum Schwarzschild radius $a_{max} = a(u_0)$ and $a_{min} = a(u_1)$. Hence we have the relations

$$\frac{r_{max}}{r_{min}} \simeq \frac{a_{max}}{a_{min}}, \quad \frac{a_{min}}{r_{min}} \simeq 1. \quad (4.20)$$

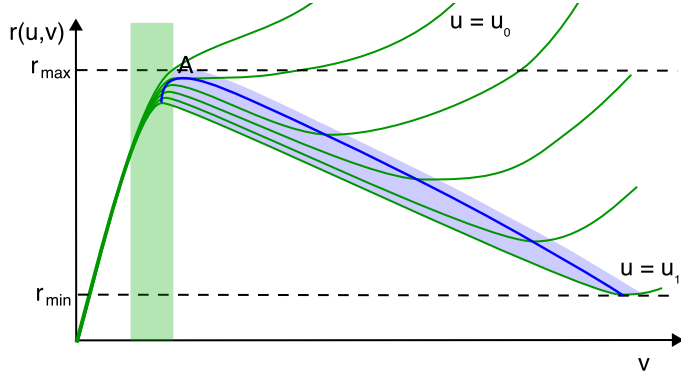


Figure 4: Schematic diagrams of $r(u, v)$ vs v . For discrete values of u , including u_0 and u_1 , $r(u, v)$ is plotted as functions of v (green curves) for given values of u . These constant- u curves almost coincide inside the collapsing matter (thick green strip), as well as in the flat spacetime inside the matter shell (on the left of the green strip). Outside the collapsing matter, the local minima of the $r(u, v)$ curves at different u (where $\partial_v r(u, v) = 0$) are located on the trapping horizon $r(u_{ah}(v), v)$ (blue curve). The near-horizon region is shown as the blue-shaded area.

We thus conclude from eqs.(4.18), (4.17) and (4.20) that

$$\Delta\Sigma \lesssim \mathcal{O}\left(\frac{n^3 \ell_p^2}{a_*^2}\right), \quad (4.21)$$

where n is defined in eq.(4.3).

Now, the function $C(u, v)$ will be important to evaluate the proper distance in the next section. In the definition of $\Sigma(u, v)$ (3.9), when we write the leading solution (4.16) as $C^{(0)}$, the correction $\Delta\Sigma$ appears as $C = C^{(0)}e^{\Delta\Sigma} \approx C^{(0)}(1 + \Delta\Sigma)$. Therefore, the condition for C to be dominated by $C^{(0)}$ is

$$\frac{C - C^{(0)}}{C^{(0)}} \approx \Delta\Sigma \ll 1. \quad (4.22)$$

Thus the evaluation (4.21) means that whenever

$$n \ll \frac{a^{2/3}}{\ell_p^{2/3}} \quad (4.23)$$

holds, the 0-th order result (4.16) is good.

5 Distance in Near-Horizon Region

Finally, we use the 0-th order solution of the metric (4.16) to compute the upper bound of the distance between the trapping horizon and the surface of the collapsing matter.

First note that the formula (4.16) can be applied to any point inside the near-horizon region. We can calculate the distance between any two points inside the region connected

through a spacelike curve \mathcal{C} restricted to the $u-v$ plane.¹⁰ The proper length along a given curve \mathcal{C} is evaluated as

$$\begin{aligned}
\Delta L &= \int_{\mathcal{C}} \sqrt{-C(u,v)} du dv \\
&\leq C^{1/2}(u_*, v_*) \frac{r^{1/2}(u_*, v_*)}{r^{1/2}(u, v)} \int_{\mathcal{C}} \sqrt{-e^{-\frac{u-u_*}{2a_{max}}} e^{-\frac{v_*-v}{2a_{max}}}} du dv \\
&\leq C^{1/2}(u_*, v_*) \frac{r_{max}^{1/2}}{r_{min}^{1/2}} \int_{\mathcal{C}} \sqrt{-dU dV} \simeq C^{1/2}(u_*, v_*) \frac{a_{max}^{1/2}}{a_{min}^{1/2}} \int_{\mathcal{C}} \sqrt{dX^2 - dT^2} \\
&\leq C^{1/2}(u_*, v_*) \frac{a_{max}^{1/2}}{a_{min}^{1/2}} \int_{\mathcal{C}} dX \leq 2 \frac{a_{max}^{3/2}}{a_{min}^{1/2}} C^{1/2}(u_*, v_*) \\
&\sim \mathcal{O}\left(\frac{a_{max}^{3/2}}{a_{min}^{3/2}} \ell_p\right) = \mathcal{O}(n^{3/2} \ell_p), \tag{5.1}
\end{aligned}$$

where we have used eqs.(4.20) and (4.17) and the definition $n \equiv a_{max}/a_{min}$. We also have introduced new coordinates (see Fig.5):

$$U = T - X = -2a_{max} e^{-\frac{u-u_*}{2a_{max}}} \in (-2a_{max}, 0), \tag{5.2}$$

$$V = T + X = 2a_{max} e^{-\frac{v_*-v}{2a_{max}}} \in (0, 2a_{max}). \tag{5.3}$$

By the same calculation, the proper time for a timelike curve is also at most of the same order of magnitude.

This result means that any proper distance in the radial direction inside the near-horizon region is bounded from above by $n^{3/2} \ell_p$. In particular, this conclusion applies to the proper distance between the trapping horizon and the surface of the collapsing matter, since both are in the near-horizon region.

At first glance, this result might seem purely classical because the 0-th order solution $C(u, v)$ (4.16) has been obtained from eq.(4.10), which includes no quantum correction. However, we have arrived at eq.(5.1) by using the inequalities (4.7), which is a consequence of the negative vacuum energy. Therefore, this result actually relies on the quantum effect.

At the Page time ($n = 2$), the distance between the collapsing matter and the trapping horizon is at most ℓ_p . When 99% of the black hole is evaporated, the distance is at most 100 times the Planck length, which is still too small to be distinguished from 0 in a low-energy effective theory such as the Standard Model. In other words, from the viewpoint of a low-energy effective theory, the surface of the collapsing matter simply coincides with the trapping horizon¹¹.

¹⁰ Each point in the $u-v$ plane represents a 2-sphere in 4D. The curve \mathcal{C} is restricted to the radial and temporal directions in 4D to define the distance between two concentric 2-spheres.

¹¹ Interestingly, another self-consistent model [9, 10], in which there is no trapped region, provides a similar result. A collapsing matter is just *above* the Schwarzschild radius by a Planckian distance. In this sense, the conventional model, which we are studying in the present paper, might eventually be close to such a model.

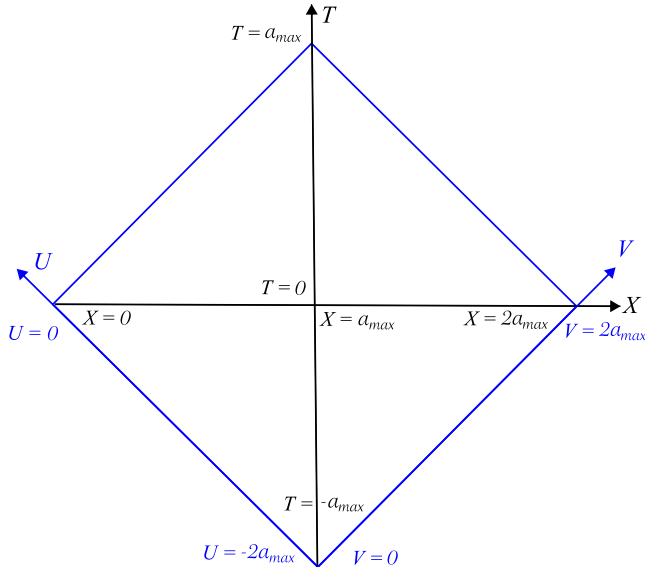


Figure 5: The near-horizon region is mapped to a subspace of the $U - V$ space via eqs.(5.2) and (5.3). The distance between any two points in the near-horizon region is shorter than the distance between their images in this diamond. Corresponding to $U \in (-2a_{max}, 0)$ and $V \in (0, 2a_{max})$, we have $X \in (0, 2a_{max})$ and $T \in (-a_{max}, a_{max})$. Within this space, the curve with maximal proper distance is the X -axis at $T = 0$, and the curve with the maximal proper time is the T -axis at $X = a_{max}$.

6 Conclusion

In the above, we have shown that during the time in which the black hole's mass is reduced to $1/n$ of its initial mass, the proper distance ΔL between the surface of the collapsing matter and the timelike trapping horizon is bounded from above by $\Delta L \leq n^{3/2}\ell_p$. This bound holds for all non-null paths along which $d\theta = d\phi = 0$. This condition is valid as long as $n \ll a^{2/3}/\ell_p^{2/3}$.

To prove this statement, we have solved the function $C(u, v)$ in the metric (2.3) from the semi-classical Einstein equation. The zero-th order solution is give by eq.(4.16):

$$C(u, v) \simeq C(u_*, v_*) \frac{r(u_*, v_*)}{r(u, v)} e^{-\int_{u_*}^u \frac{du'}{2a(u')} - \int_{v_*}^v \frac{dv'}{2\bar{a}(v')}} \tag{6.1}$$

which is independent of the details of the vacuum energy-momentum tensor. It is a good approximation under the assumptions listed in Sec.2.

The other function $r(u, v)$ in the metric (2.3) depends on more details about the vacuum energy-momentum tensor ¹². The only feature about $r(u, v)$ needed to derive the upper

¹²We can use a 2D model and calculate $r(u, v)$ explicitly [7]. We can see the same result about the short distance and show that the curvature is small.

bound (5.1) on ΔL is the relation (4.20), which is a consequence of the structure that the near-horizon region is mostly inside the trapped region.

Finally, it would be interesting to investigate implications of the extremely small distance between the matter and the horizon for the information paradox [18].

Acknowledgement

We thank Hikaru Kawai for valuable discussions and suggestions. P.M.H. thanks iTHEMS at RIKEN, University of Tokyo and Kyoto University for their hospitality during his visits where the major part of this work was done. P.M.H. is supported in part by the Ministry of Science and Technology, R.O.C. and by National Taiwan University. The work of Y.M. is supported in part by JSPS KAKENHI Grants No. JP17H06462. Y.Y. is partially supported by Japan Society of Promotion of Science (JSPS), Grants-in-Aid for Scientific Research (KAKENHI) Grants No. 18K13550 and 17H01148. Y.Y. is also partially supported by RIKEN iTHEMS Program.

References

- [1] S. D. Mathur, “The Information paradox: A Pedagogical introduction,” *Class. Quant. Grav.* **26**, 224001 (2009) [arXiv:0909.1038 [hep-th]].
- [2] A. Almheiri, D. Marolf, J. Polchinski and J. Sully, “Black Holes: Complementarity or Firewalls?,” *JHEP* **1302**, 062 (2013) [arXiv:1207.3123 [hep-th]];
- [3] S. L. Braunstein, “Black hole entropy as entropy of entanglement, or it’s curtains for the equivalence principle,” [arXiv:0907.1190v1 [quant-ph]] published as S. L. Braunstein, S. Pirandola and K. yczkowski, “Better Late than Never: Information Retrieval from Black Holes,” *Phys. Rev. Lett.* **110**, no. 10, 101301 (2013), for a similar prediction from different assumptions.
- [4] P. C. W. Davies, S. A. Fulling and W. G. Unruh, “Energy-momentum Tensor Near an Evaporating Black Hole,” *Phys. Rev. D* **13**, 2720 (1976). doi:10.1103/PhysRevD.13.2720
- [5] S. M. Christensen and S. A. Fulling, “Trace Anomalies and the Hawking Effect,” *Phys. Rev. D* **15**, 2088 (1977). doi:10.1103/PhysRevD.15.2088

- [6] R. Brout, S. Massar, R. Parentani and P. Spindel, “A Primer for black hole quantum physics,” *Phys. Rept.* **260**, 329 (1995) doi:10.1016/0370-1573(95)00008-5 [arXiv:0710.4345 [gr-qc]].
- [7] P. M. Ho, Y. Matsuo, Y. Yokokura, “An Analytic Description of Semi-Classical Black-Hole Geometry” [arXiv: 1912.*****[hep-th]].
- [8] S. A. Fulling, “Radiation and Vacuum Polarization Near a Black Hole,” *Phys. Rev. D* **15**, 2411 (1977). doi:10.1103/PhysRevD.15.2411
- [9] H. Kawai, Y. Matsuo and Y. Yokokura, “A Self-consistent Model of the Black Hole Evaporation,” *Int. J. Mod. Phys. A* **28**, 1350050 (2013) [arXiv:1302.4733 [hep-th]].
- [10] H. Kawai and Y. Yokokura, “A Model of Black Hole Evaporation and 4D Weyl Anomaly,” *Universe* **3**, no. 2, 51 (2017) doi:10.3390/universe3020051 [arXiv:1701.03455 [hep-th]].
- [11] I. Booth, “Black hole boundaries,” *Can. J. Phys.* **83**, 1073 (2005) doi:10.1139/p05-063 [gr-qc/0508107].
- [12] J. Thornburg, “Event and apparent horizon finders for 3+1 numerical relativity,” *Living Rev. Rel.* **10**, 3 (2007) [gr-qc/0512169].
- [13] V. Faraoni, “Evolving black hole horizons in General Relativity and alternative gravity,” *Galaxies* **1**, no. 3, 114 (2013) doi:10.3390/galaxies1030114 [arXiv:1309.4915 [gr-qc]].
- [14] V. P. Frolov and G. A. Vilkovisky, “Spherically Symmetric Collapse in Quantum Gravity,” *Phys. Lett. B* **106**, 307 (1981).
- [15] T. A. Roman and P. G. Bergmann, “Stellar collapse without singularities?,” *Phys. Rev. D* **28**, 1265 (1983). doi:10.1103/PhysRevD.28.1265
- [16] S. A. Hayward, “Formation and evaporation of regular black holes,” *Phys. Rev. Lett.* **96**, 031103 (2006) [gr-qc/0506126].
- [17] P. M. Ho and Y. Matsuo, “Trapping Horizon and Negative Energy,” *JHEP* **1906**, 057 (2019) doi:10.1007/JHEP06(2019)057 [arXiv:1905.00898 [gr-qc]].
- [18] P. M. Ho and Y. Yokokura, to appear.